Scaling Properties of L-band Passive Microwave Soil Moisture: From SMOS to Paddock Scale

Rocco Panciera[1], Jeffrey P. Walker[1], Olivier Merlin[1], Jetse D. Kalma[2] and Edward J. Kim[3]

1 Department of Civil and Environmental Engineering, University of Melbourne, Australia
2 School of Engineering, University of Newcastle, Australia
3 NASA Goddard Space Flight Center, Greenbelt, USA

Abstract: Remote sensing of soil moisture is a powerful and inexpensive way to map surface soil moisture for a range of applications, including weather prediction, water resources management and irrigation practices. Passive microwave sensors operating at L-band wavelength have shown the most potential for this task. However, this technology faces some major challenges, mostly related to correct interpretation of the spatially averaged measurements provided by such sensors and the mismatch between typical observation scales at L-band (50km) and the resolution at which data are needed for many environmental applications (1km). Due to the imminent launch (2007) of the first dedicated soil moisture mission, the European passive microwave Soil Moisture and Ocean Salinity (SMOS) satellite, it is important to address these issues by investigating the effect of sub-pixel variability in soil moisture and land surface features (vegetation cover, soil type, soil temperature) on radiobrightness observations, so that suitable downscaling schemes may be developed. The National Airborne Field Experiment 2005 (NAFE'05) conducted in the Goulburn catchment was designed with this primary objective. The NAFE'05 dataset is unique worldwide due to the wide range of spatial scales at which passive microwave observations were made, ranging from 1km to 62.5m resolution. Supporting ground measurements were also made at a range of scales from 1km to 6.25m resolution. In this study, airborne observations from the NAFE'05 campaign are used to examine the scaling properties of L-band passive microwave signatures across scales from 1km to 62.5m. The spatial properties of passive microwave signatures are compared across multiple observation scales. High resolution observations are also spatially aggregated and compared with the microwave signature as observed at subsequently lower resolutions. Results indicate a limited impact of land surface variability on the scaling behaviour of brightness temperatures, with the area-averaged brightness temperature measured at different resolutions varying of less then 6K.

Keywords: Remote sensing, L-band, Passive microwave, SMOS, Soil moisture, Scaling

1. INTRODUCTION

Remote sensing has a unique potential for providing frequent observations of near-surface soil moisture over large regions, thus overcoming the intrinsic problems of traditional ground based measurement of soil moisture profile (Schmugge at al., 1980; Jackson 1993). However, state-of-the-art L-band passive microwave technology faces a number of problems related to: (i) the correct interpretation of the large-scale spatially averaged passive microwave observations provided by the remote sensor (generally referred to as brightness temperatures), which for satellite applications is about 50km; (ii) the inconsistency between the scales at which the variables are measured and predictions are needed; and (iii) the applicability of soil moisture retrieval algorithms from brightness temperatures developed using radiometers mounted on towers or trucks, whose field of view is limited to 10's of meters, to satellite sensors characterised by large footprints. To resolve these issues, a good understanding of the scaling properties of L-band passive microwave observations is imperative.

An extensive airborne campaign named the National Airborne Field Experiment (NAFE) was conducted in South-Eastern Australia in 2005, with the specific purpose to address these scaling issues. The data from this experiment are presented here for the first time, and an initial scaling analysis performed over a portion of the dataset discussed. The purpose of this study is to analyse the effect of spatial resolution and land surface characteristics on brightness temperature fields. This study is unique in that it utilises optimal instrument configuration for soil moisture retrieval, and

independent, concurrent observation of the same area at different resolutions.

2. EXPERIMENT DESCRIPTION

The brigthness temperature observations used in this study have been collected during the month-long NAFE field campaign, held in November 2005. The campaign included extensive airborne passive microwave observations together with spatially distributed and in-situ ground monitoring of soil moisture. For the purpose of this analysis, only the airborne data and the radiometer used in this study will be described here.

2.1 The airborne data

The study area is situated in the northern part of the Goulburn River catchment, located in a semiarid area of south-eastern Australia. The area monitored during NAFE'05 was a square of approximately 40kmx40km, centred in the northern part of the catchment. This area was logistically divided into two sub-areas, the "Merriwa" area in the right side of the square and the "Krui" area in its left side (see Figure1).

Flights were conducted between October 31 and November 25 with a small two-seater motor glider from the Airborne Research Australia national facility together with the recently acquired Polarimetric L-band Multi-beam Radiometer (PLMR). The PLMR measures both

Figure 1. The NAFE'05 study area in the Goulburn catchment. "R" indicates the area covered by regional flights, while "K" and "M" define the Krui and Merriwa focus areas. Focus farms and soil moisture stations are also shown.

V and H polarised brightness temperature (T_b) using a single receiver with polarisation switch at incidence angles +/-7°, +/-21.5° and +/-38.5° in either across track (push-broom) or along track configurations. The payload also included a thermal imager. A digital camera and tri-spectral scanner were also used to map the whole study area on one occasion.

Multi-resolution flights were undertaken with the PLMR instrument in "push-broom" configuration to satisfy a major objective of the experiment. The area mapped on each date was either the Krui or the Merriwa area, alternatively. Flying at 4 different altitudes over the same area resulted in 4 ground resolutions: (i) 1km (L), (ii) 500m (M), (iii) 250m (H) and (iv) 62.5m (VH) footprint sizes. The area was entirely mapped at a particular altitude before descending to subsequently lower altitudes.

On multi-resolution flights, full coverage of the same ground area was always guaranteed at each resolution. Furthermore, to avoid gaps in the data due to anomalous aircraft attitude or the terrain elevation effect on the swath, a full one-pixel wide overlap was guaranteed for adjacent flight lines on all "push-brooms" flights.

Three dates were selected for this analysis from the extensive NAFE'05 datasets: November 1, 10 and 17, respectively, being at the beginning, the middle and toward the end of the field campaign. These dates are representative of the conditions the study area underwent during the campaign: very wet on November 1 after a heavy thunderstorm on October 31 and then gradually drier towards the end of the campaign.

3. PREPROCESSING OF PLMR DATA

The standard PLMR data output of T_b were georeferenced at both polarisations, and internally calibrated against cold and warm loads. These raw data were further calibrated daily during the campaign, with a 4 point calibration against two "ground" targets, one cold and one warm, both before and after the flight. Specific daily calibration coefficients were applied for each beam and polarisation.

The main objective of this study was the comparison of T_b at different resolutions. Ideally, observations are of the same area, at the same time of the day, with the same instrument configuration. In reality, the T_b observations available have been taken at different view angles and different times of the day, when the soil temperature might be
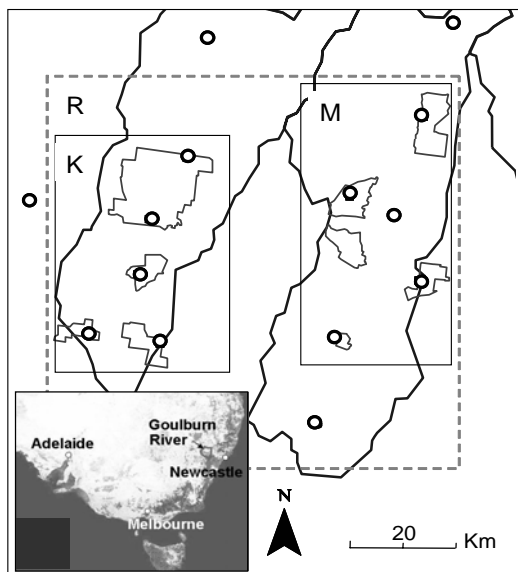
significantly different. Therefore, it is necessary to normalise the observation to the same view angle and soil temperature.

To account for diurnal changes of effective soil temperature on the observed T_b, the shallow temperature measurements at the monitoring stations were used. For each PLMR acquisition, the ratio between the actual soil temperature and a reference (10:00 AM) soil temperature was used to normalise the actual T_b.

Normalisation for the view angle was done by assuming that for a given day, flight line and instrument beam, the view angle effect on T_b, described by the Fresnel equation, is constant for the range of soil moisture and vegetation present. Figure 2 shows the average T_b values for each PLMR beam as a function of beam angle and date for the whole Krui sub-area. The pattern of variation reflects the Fresnel effect. Notice the consistent symmetry about nadir, which indicates little or no instrumental effect on the angular response. For each beam, a normalisation factor was computed as the ratio between the daily average T_b for the view angle taken as reference (21.5°) and the daily average T_b for the specific beam of interest.

4. RESULTS AND ANALYSIS

To analyse the relationship between T_b data collected at different spatial resolutions, the following analysis were undertaken:

- Visual comparison of T_b images at different resolutions;
- Statistical comparison between T_b fields at different resolutions;
- Pixel-by-pixel comparison of aggregated high resolution T_b and low resolution T_b.

4.1 Visual comparison

To facilitate comparison between different resolutions, PLMR data were binned into reference grids with nominal cell sizes corresponding to the nominal PLMR resolution for that altitude. The corresponding value of T_b for each cell was then calculated by linearly averaging all the temperature and incidence angle corrected beams whose centroid fell within that cell.

An example of the resulting multi-resolution maps is shown in Figure 3 for the three dates considered in this study. The images are relative to the Krui study areaed The general site layout is also shown in Figure 3, with a

Landsat Thematic Mapper image of the area and the 250m Digital Elevation Model. The topography of the area is characterised by the steep Liverpool ranges in the north-west part of the area to the flat Merriwa Plateau in the south. The Landsat image shows areas covered by forest or open woodland (dark grey) in the south [fig4 should be "Landsat"] of the area and on the hills of the Ranges. Light grey coloured areas correspond to crops and native grass.

The consistency between patterns of T_b at different resolutions and in time is notable. The topographically elevated northern and central areas present consistently lower values of T_b than the valley bottom crossing the upper part of the image in a roughly NE-SW direction, and the southern plateau. Sharp contrasts in T_b are also due to irregular rainfall distribution over the area on various occasions; eg. heavy thunderstorms were experienced on October 31. The patterns are well visible at low resolution, and consistent between dates. For example, the period between November 1 and November 10 was dry with only minor rainfall, and this is reflected in the general increase of T_b in response to drying. Vegetation effects are also readily observed near the forest in the south part of the area, which shows higher values of T_b for increased vegetation density. This pattern is also visible in the low resolution images and is consistent across dates.

Comparison between VH and L resolution also shows how some high resolution T_b patterns that correspond to fine scale land surface features which are not readily observed at low resolution. Consider for example the extreme top right corner of the images in panel a). The diagonal wetter feature visible in the VH and H image corresponds to the alluvial areas around the Krui River, and it is coupled with an
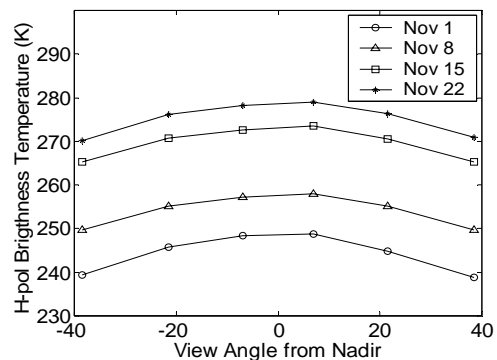

Figure 2. View angle effect on H polarisation brightness temperatures.
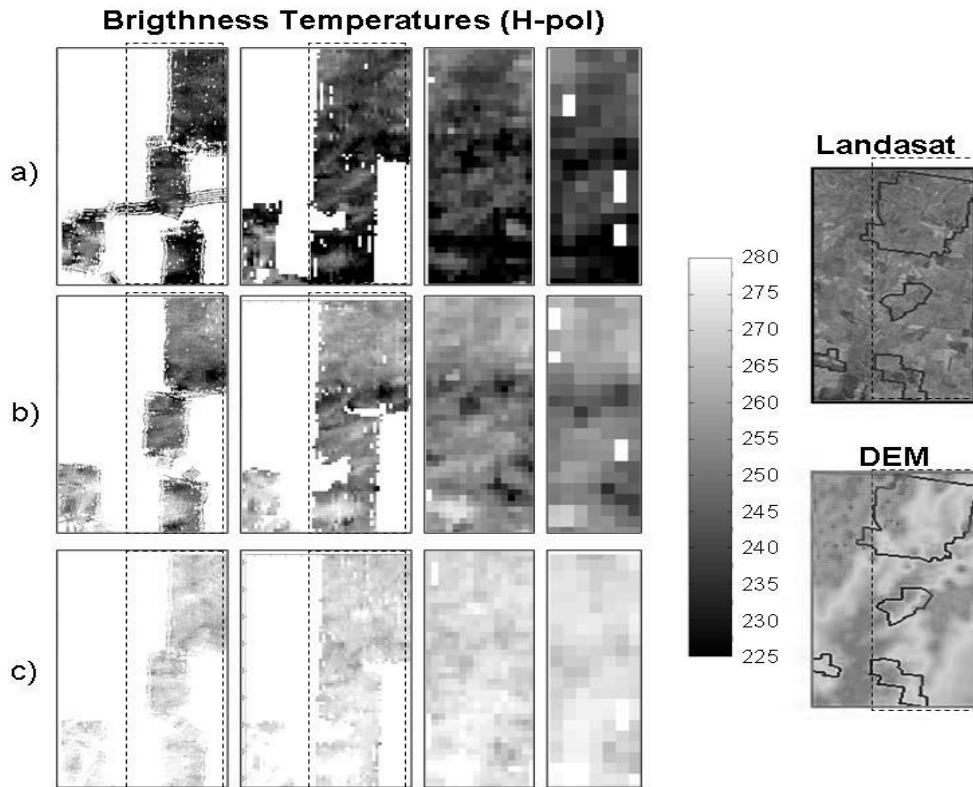
Brigthness Temperatures (H-pol)

Figure 3. H polarised brightness temperatures for (a) November 1, (b) November 10 and (c) November 17. Resolution decreases from left to right, 62.5m (VH), 250m (H), 500m (M) and 1km (L) respectively. The boundaries of the M and L mapping in the VH and H maps are indicated as a dotted square.

adjacent area of higher T_b associated with a hilltop. These features are not observed in the L image. Although the difference in T_b between the two areas is still visible, the gradient is smoother. These images show how as the resolution of observation decreases the main spatial features of T_b distribution are retained, but generalised and smoothed.

4.2   Statistical analysis

By normalising the brightness temperature data to 10am and 21.5° incidence angle, the T_b data observed at different altitudes are directly comparable. In this section the statistical properties of the T_b fields are compared across observation resolutions.

In Figure 4 the distribution of T_b are shown for each date and each resolution. It is readily observed that T_b can be fairly well described by a normal distribution about the mean value. The distributions are shifted toward higher T_b values for November 10 and 17, which is consistent with the wetter soil moisture conditions. Moreover, the peakedness of the curves is

higher for the drier conditions, due to the lower spatial variability observed in dry soil moisture.

These characteristics are clearly retained across the various observation resolutions, confirming that low resolution observations are able to capture to a certain degree the trends in wetness conditions and degree of spatial variability indicated by high resolution values. In Table 1, the statistical properties of these T_b distributions are summarised for the three dates. In each case, the mean T_b observed at different altitudes is very close for the various resolutions, differing by less then 6K. This is encouraging, although it's unclear why this mean consistently increases with decreasing pixel size. This might be an effect of the data processing, such as the correction for temperature changes, as well as some instrumental effect which could cause a decrease of the antenna response in time (as the altitudes are covered downward). More refined data processing and extension of the analysis to the whole dataset will give a better idea about the persistence of this effect. Notably the difference between mean T_b at multiple resolutions is smaller for drier
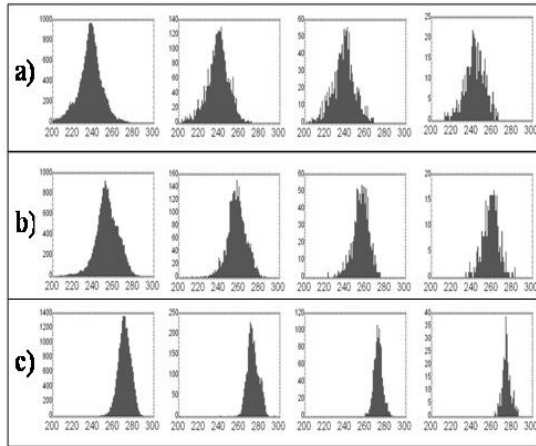
Figure 4. Brightness temperatures distribution for 4 different resolution observations and 3 dates: November 1 (panel a), November 10 (panel b) and November 17 (panel c). Resolution decreases from left to right, 62.5m, 250m, 500m and 1km respectively.

conditions, where the soil signature on the microwave signal is expected to be higher with respect to vegetation attenuation.

Both the standard deviation and the range of T_b decrease slightly with resolution. Although the range of T_b values is nearly double at 62.5m resolution with respect to 1km resolution, the variation in standard deviation is smaller, on the order of 2-3K. Although this can be partially due to the lower spatial variability observed at lower resolution, it is likely to be highly affected by extreme values of T_b (like small water bodies, vegetation patches) which are captured by high resolution data and are averaged in the low resolution observations. In this sense it is interesting to notice how on two of the three dates considered the standard deviation and range of T_b observed at different altitudes have a sharp maximum at 250m resolution (Table 2). Extension of the analysis to the whole dataset is needed to understand wether this effect is consistently observed and wether it has a significant meaning in terms of optimal observation resolution.

Statistical analysis therefore indicates that while there is a loss in spatial detail when decreasing the resolution at which T_b are observed, the average T_b value measured over the whole area is constant across resolutions, differing by less then 6K across 3 orders of magnitude in resolution. For L-band soil moisture retrieval under moderate vegetation conditions, this corresponds to approximately 2% V/V moisture content difference. This preliminary result

therefore suggests a limited impact of the sub-pixel spatial variability of land surface features on the retrieval of an average value of soil moisture content from passive microwave signatures for a large area. It also points toward the applicability of soil moisture passive microwave retrieval algorithms developed from tower-based radiometers at resolutions typical of aircraft monitoring.

4.3   Pixel-by-pixel comparison

A third step of the analysis was to compare the averaged high resolution T_b to the low resolution observations collected over the entire area on a pixel-by-pixel basis. Given that the land surface conditions will generally vary from pixel to pixel, and that these are known for the area of interest, this analysis is useful to understand how different land surface distributions impact the area-averaged T_b.

For this experiment, the T_b for each pixel at each resolution was compared with the T_b observed at higher resolutions aggregated within the pixel. The results for November 1 (wet conditions) are shown in Figure 5. Each plot shows the comparison of each T_b pixel against the higher resolution, area-averaged value within that pixel A linear regression is also shown to help interpret the data.

The comparison shows excellent correlation between T_b observed and aggregated for each pixel at all resolutions and "aggregation ratio" (i.e., the ratio between the pixel size of the aggregated observations and the "comparison" pixel size). This indicates a linear scaling character of passive microwave signatures across most land surface conditions.

A slight and consistent deviation from a fully linear scaling is readily observed in all cases,

Table 2. Statistical properties of the T_b distribution shown in Figure 4.

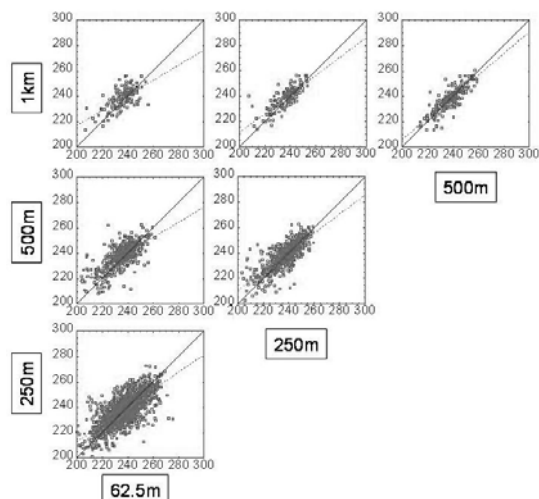| Date	Pixel size (m)	Mean (K)	Stdev (K)	Range (K)
1-Nov	1000	243.43	10.08	53.02
	500	238.90	11.09	66.23
	250	239.05	11.32	93.05
	62.5	237.31	12.20	125.02
10-Nov	1000	259.49	8.17	48.67
	500	256.32	8.11	52.47
	250	257.75	15.19	274.68
	62.5	254.49	11.16	171.61
17-Nov	1000	275.13	4.27	23.30
	500	273.42	4.23	26.90
	250	273.78	10.79	281.33
	62.5	271.88	6.32	67.12

Figure 5. Correlation between high resolution aggregated T_b (column footers) and independent low resolution observations (row headers).

considered as difference in the scaling between dry and wet pixels. Amongst wet pixels (i.e. lower T_b) the agreement between aggregated T_b and lower resolution T_b is poorer, as particularly evident in the first two panels of row 1 and 2 in Figure 5. Such behaviour is consistent amongst the cases considered in this study, and is more evident with increasing aggregation ratio (see row 1 in Figure 5). This indicates that at low moisture content, when the soil signature on T_b is weaker with respect to other factors (eg. Vegetation), the distribution of land surface features might play an important role in determining non-linear scaling of the passive microwave signal. These conclusions need verification through extension of the analysis to the whole NAFE'05 datasets.

5.   CONCLUSIONS

This study presented a preliminary analysis of the unique NAFE'05 dataset, whose major component is represented by L-band passive microwave observations at multiple resolutions. The aim was to understand whether independent brightness temperature observations of the same area at different resolutions result in the same averaged brightness temperature, and how the land surface variability impacts the area-average brightness temperature.

The distribution of brightness temperatures over the study area clearly reflected by surface characteristics like topography, vegetation and soil moisture, although spatial features are smoothed at lower resolutions. Statistical comparison between resolutions showed that

the area-averaged brightness temperature remains fairly constant, within 6K. The same comparison made on a pixel-by-pixel basis indicated excellent overall correlation between observations at different resolutions.

These preliminary results point toward the applicability of soil moisture passive microwave retrieval algorithms developed from tower-based radiometer at lower resolutions. Nevertheless, indications of a non linear scaling of passive microwave signatures on wet land surface conditions are drawn and give direction sfor future investigations and extension of the analysis to the entire NAFE'05 dataset.

6.   ACKNOWLEDGEMENTS

7.   REFERENCES

Jackson, T.J., Measuring surface soil moisture using passive microwave remote sensing. *Hydrological Processes* 7, 139-152, 1993.

Schmugge, T.J., et al., Survey of Methods for Soil Moisture determination. *Water Resources Research* 16, 961-979, 1980.

Jackson, T.J., et al., Passive microwave remote sensing of soil moisture from an aircraft platform. *Remote Sensing of Environment* 14, 135-151, 1984.

Jackson, T.J., et al., Passive Microwave Sensing of Soil-Moisture under Vegetation Canopies. *Water Resources Research* 18, 1137-1142, 1982.

Jackson, T. J., Multiple Resolution Analysis of L-Band Brightness Temperature for Soil Moisture. *IEEE Transaction on Geoscience and Remote Sensing* 39, 1,151-164, 2001.

Wang, J.R., Passive microwave sensing of soil moisture content: The effects of soil bulk density and surface roughness. *Remote Sensing of Environment* 13, 329-344, 1983.

Drusch, M., et al., Up-scaling effects in passive microwave remote sensing: ESTAR 1.4 GHz measurements during SGP'97. *Geophys. Res. Lett.* 26, 879-882, 1999.